The Journal of Open Source Software

atems: Analysis tools for TEM images of carbonaceous particles

Timothy A Sipkens [1,2¶], **Ramin Dastanpour** [1], **Una Trivanovic** [1], **Hamed Nikookar** [1], **and Steven N. Rogak** [1]

1 Mechanical Engineering, University of British Columbia, Canada **2** Metrology Research Centre, National Research Council Canada, Canada ¶ Corresponding author

DOI: 10.xxxxxx/draft

Software

- Review
- Repository
- Archive

Editor: Open Journals

Reviewers:

- @openjournals

Submitted: 01 January 1970
Published: unpublished

Summary

The objective of atems is to provide a suite of open source analysis tools (largely in Matlab) for transmission electron microscopy (TEM) image analysis that are specifically designed for soot and related carbonaceous particles (e.g., tarballs). This codebase started as a manual analysis code by Dastanpour & Rogak (2014), with the first automated methods added by Dastanpour et al. (2016). The current, open source version has been streamlined and expanded to include a larger suite of automated analysis methods from the literature, as detailed in the following section. In this regard, a key contribution of this codebase is to provide open source implementations of multiple analysis methods spanning a range of laboratories. This codebase places these methods in the same framework, with the goal of enabling intercomparisons of analysis routines across a range of data.

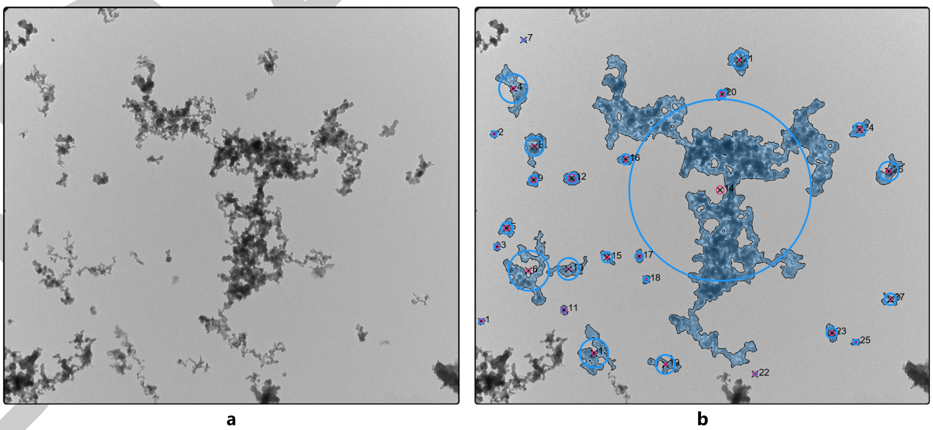

Figure 1: Sample TEM image of soot demonstrating the aggregate structure, where **a** is an unlabeled image containing soot aggregates and **b** is that same image with the aggregates labeled.

Statement of need

Soot, carbon black, and other carbonaceous particles have important climate, health, and technological impacts that depend on their morphology. These particles have complex shapes composed of a collection of small, primary particles in fractal arrangements, as shown in Figure 1a. TEM images of these particles allow for detailed information about particle morphology that is unavailable in other characterization techniques. However, extracting this information requires image analysis across a statistically-significant number of particles,

The Journal of Open Source Software

with the quality of conclusions improving as the number of characterized particles increases. For instance, Kelesidis et al. (2020) suggested quantifying at least 400 primary particles per experimental condition in a premixed flame to get an accurate average primary particle diameter from manually drawing elipses (that study counted 800 primary particles). In the broader literature, a few hundred particles per condition seems to be standard, with other authors having employed between 150 and 400 particles per condition (Liati et al., 2014; Marhaba et al., 2019; Trivanovic et al., 2019, 2020), depending on the type of analysis. For multiple conditions, this can quickly expand to over 1000 particles. This characterization is often done manually, which at a minimum of several minutes per aggregate, is incredibly labour intensive. Unfortunately, the low contrast (carbonaceous particles on carbon films) and complex particle morphology of common carbonaceous particles makes automated analysis challenging, requiring unique analysis methods over those developed for traditional TEM image analysis of many engineered nanomaterials (Schneider et al., 2012). At the same time, existing automated methods across the literature are typically only applied to data from a single laboratory, with few exceptions (Anderson et al., 2017; Sipkens et al., 2021). This limits comparability between laboratories (Sipkens et al., 2023).

Methods

After loading images (with an automated method provided for doing so), analysis involves two major steps.

The first step is segmentation of the aggregates from their background. Available methods include the slider-based manual approach of Dastanpour & Rogak (2014); the common Otsu method; a modification of Otsu by Dastanpour et al. (2016) that employs morphological operations to improve segmentation; the *k*-means approach of Sipkens & Rogak (2021); and `carboseg`, which is the convolutional neural network (CNN) approach from Sipkens et al. (2021). Functionality is also available to prepare (e.g., read and crop image footers) and export images for external analysis, prior to reading the images in for subsequent analysis. This enables external extensions, such as the WEKA segmentation method of Altenhoff et al. (2020). Tools are then available to compute aggregate projected area, perimeter, and circularity, among other properties. A sampling of segmentations produced by these methods is presented in Figure 2.

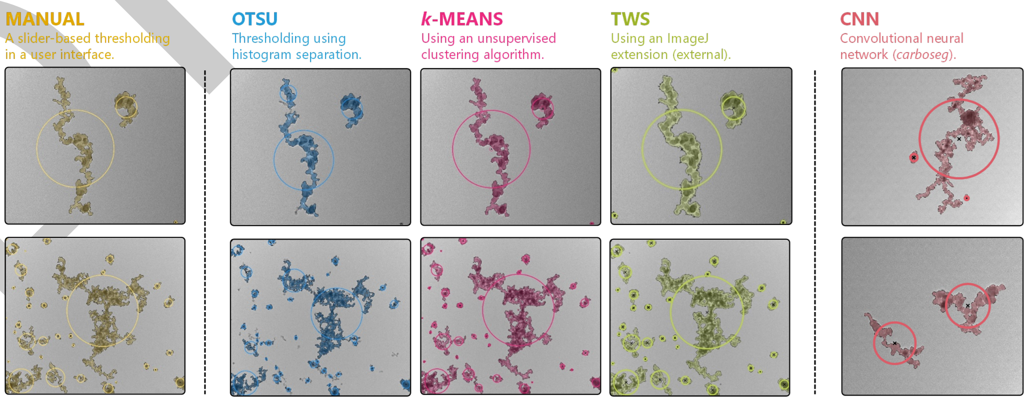

Figure 2: Sample segmentations across a range of methods available in this code. The manual method corresponds to an updated version of the code development by Dastanpour et al. (2016). The Otsu segmentation is standard Otsu, without any adaptations. The *k*-means method is that described by Sipkens & Rogak (2021). TWS refers to trainable WEKA segmentation based on the method described by Altenhoff et al. (2020), which makes use of the code enabling external extensions. These first four panels correspond to images from Sipkens & Rogak (2021). The final panel corresponds to the convolutional neural network method described by Sipkens et al. (2021).

Second, this code works to identify primary particles, that is the small, roughly circular structures inside the aggregates. Available methods include a updated version of the Euclidean distance mapping–surface-based scale analysis (EDM-SBS) of Bescond et al. (2014), converted from SciLab to Matlab in association with Sipkens et al. (2021) (functionality between the two languages resulted in minor differences); the Euclidean distance mapping–watershed (EDM-WS) method of De Temmerman et al. (2014); the pair correlation method (PCM) of Dastanpour et al. (2016); the Hough transform method of Kook et al. (2016); and the Hough transform method of Altenhoff et al. (2020).

General plotting and other utilities (`tools.*`) are provided to enable further analysis and visualization (e.g., as in Figure 1b and Figure 2).

Use

This code has been used in a number of studies in the literature. This code was used by Sipkens et al. (2021) to compare multiple segmentation and primary particle analysis methods. The code was also used by Trivanovic et al. (2019), Kheirkhah et al. (2020), and Trivanovic et al. (2020) to perform image analysis of marine engine and flare soot. The *k*-means method in this code (Sipkens & Rogak, 2021) was also employed for soot by Li (2022).

Acknowledgements

We wish to acknowledge related code released in association with some of the cited work. These including Matlab code provided in Kook et al. (2016) and SciLab code released in association with Bescond et al. (2014). The code from Altenhoff et al. (2020) was provided by the authors and adapted to the present format.

We also wish to acknowledge funding by the Canadian Council of the Arts (Killam Fellowship), the Natural Sciences and Engineering Research Council of Canada (NSERC), and Transport Canada.

References

Altenhoff, M., Aßmann, S., Teige, C., Huber, F. J. T., & Will, S. (2020). An optimized evaluation strategy for a comprehensive morphological soot nanoparticle aggregate characterization by electron microscopy. *Journal of Aerosol Science*, *139*, 105470. https://doi.org/10.1016/j.jaerosci.2019.105470

Anderson, P. M., Guo, H., & Sunderland, P. B. (2017). Repeatability and reproducibility of TEM soot primary particle size measurements and comparison of automated methods. *Journal of Aerosol Science*, *114*, 317–326. https://doi.org/10.1016/j.jaerosci.2017.10.002

Bescond, A., Yon, J., Ouf, F. X., Ferry, D., Delhaye, D., Gaffié, D., Coppalle, A., & Rozé, C. (2014). Automated determination of aggregate primary particle size distribution by TEM Image Analysis: Application to soot. *Aerosol Science and Technology*, *48*(8), 831–841. https://doi.org/10.1080/02786826.2014.932896

Dastanpour, R., Boone, J. M., & Rogak, S. N. (2016). Automated primary particle sizing of nanoparticle aggregates by TEM image analysis. *Powder Technology*, *295*, 218–224. https://doi.org/10.1016/j.powtec.2016.03.027

Dastanpour, R., & Rogak, S. N. (2014). Observations of a correlation between primary particle and aggregate size for soot particles. *Aerosol Science and Technology*, *48*(10), 1043–1049. https://doi.org/10.1080/02786826.2014.955565

De Temmerman, P.-J., Verleysen, E., Lammertyn, J., & Mast, J. (2014). Semi-automatic size measurement of primary particles in aggregated nanomaterials by transmission electron microscopy. *Powder Technology*, *261*, 191–200. https://doi.org/10.1016/j.powtec.2014.04.040

Kelesidis, G. A., Kholghy, M. R., Zuercher, J., Robertz, J., Allemann, M., Duric, A., & Pratsinis, S. E. (2020). Light scattering from nanoparticle agglomerates. *Powder Technology*, *365*, 52–59. https://doi.org/10.1016/j.powtec.2019.02.003

Kheirkhah, P., Baldelli, A., Kirchen, P., & Rogak, S. (2020). Development and validation of a multi-angle light scattering method for fast engine soot mass and size measurements. *Aerosol Science and Technology*, *54*(9), 1083–1101. https://doi.org/10.1080/02786826.2020.1758623

Kook, S., Zhang, R., Chan, Q. N., Aizawa, T., Kondo, K., Pickett, L. M., Cenker, E., Bruneaux, G., Andersson, O., Pagels, J., & Z., N. E. (2016). Automated detection of primary particles from transmission electron microscope (TEM) images of soot aggregates in diesel engine environments. *SAE International Journal of Engines*, *9*(1), 279–296. https://doi.org/10.4271/2015-01-1991

Li, Y. (2022). *Flame and smoke characterization in reduced gravity for enhanced spacecraft safety* [PhD thesis]. Sorbonne Université.

Liati, A., Brem, B. T., Durdina, L., Vögtli, M., Arroyo Rojas Dasilva, Y., Dimopoulos Eggenschwiler, P., & Wang, J. (2014). Electron microscopic study of soot particulate matter emissions from aircraft turbine engines. *Environmental Science & Technology*, *48*(18), 10975–10983. https://doi.org/10.1021/es501809b

Marhaba, I., Ferry, D., Laffon, C., Regier, T. Z., Ouf, F.-X., & Parent, P. (2019). Aircraft and MiniCAST soot at the nanoscale. *Combustion and Flame*, *204*, 278–289. https://doi.org/10.1016/j.combustflame.2019.03.018

Schneider, C. A., Rasband, W. S., & Eliceiri, K. W. (2012). NIH image to ImageJ: 25 years of image analysis. *Nature Methods*, *9*(7), 671–675. https://doi.org/10.1038/nmeth.2089

Sipkens, T. A., Boies, A., Corbin, J. C., Chakrabarty, R. K., Olfert, J. S., & Rogak, S. N. (2023). Overview of methods to characterize the mass, size, and morphology of soot. *Journal of Aerosol Science*, *173*, 106211. https://doi.org/10.1016/j.jaerosci.2023.106211

Sipkens, T. A., Frei, M., Baldelli, A., Kirchen, P., Kruis, F. E., & Rogak, S. N. (2021). Characterizing soot in TEM images using a convolutional neural network. *Powder Technology*, *387*, 313–324. https://doi.org/10.1016/j.powtec.2021.04.026

Sipkens, T. A., & Rogak, S. N. (2021). Using k-means to identify soot aggregates in transmission electron microscopy images. *Journal of Aerosol Science*, *152*, 105699. https://doi.org/10.1016/j.jaerosci.2020.105699

Trivanovic, U., Corbin, J. C., Baldelli, A., Peng, W., Yang, J., Kirchen, P., Miller, J. W., Lobo, P., Gagné, S., & Rogak, S. N. (2019). Size and morphology of soot produced by a dual-fuel marine engine. *Journal of Aerosol Science*, *138*, 105448. https://doi.org/10.1016/j.jaerosci.2019.105448

Trivanovic, U., Sipkens, T. A., Kazemimanesh, M., Baldelli, A., Jefferson, A. M., Conrad, B. M., Johnson, M. R., Corbin, J. C., Olfert, J. S., & Rogak, S. N. (2020). Morphology and size of soot from gas flares as a function of fuel and water addition. *Fuel*, *279*, 118478. https://doi.org/10.1016/j.fuel.2020.118478